Multiscale Model. Simul.
Vol. 9, No. 4, pp. 1373–1398

LOCALIZED BASES FOR FINITE-DIMENSIONAL HOMOGENIZATION APPROXIMATIONS WITH NONSEPARATED SCALES AND HIGH CONTRAST*

HOUMAN OWHADI† AND LEI ZHANG‡

Abstract. We construct finite-dimensional approximations of solution spaces of divergence-form operators with L^∞-coefficients. Our method does not rely on concepts of ergodicity or scale-separation, but on the property that the solution space of these operators is compactly embedded in H^1 if source terms are in the unit ball of L^2 instead of the unit ball of H^{-1}. Approximation spaces are generated by solving elliptic PDEs on localized subdomains with source terms corresponding to approximation bases for H^2. The H^1-error estimates show that $\mathcal{O}(h^{-d})$-dimensional spaces with basis elements localized to subdomains of diameter $\mathcal{O}(h^\alpha \ln \frac{1}{h})$ (with $\alpha \in [\frac{1}{2}, 1)$) result in an $\mathcal{O}(h^{2-2\alpha})$ accuracy for elliptic, parabolic, and hyperbolic problems. For high-contrast media, the accuracy of the method is preserved, provided that localized subdomains contain buffer zones of width $\mathcal{O}(h^\alpha \ln \frac{1}{h})$, where the contrast of the medium remains bounded. The proposed method can naturally be generalized to vectorial equations (such as elasto-dynamics).

Key words. homogenization, localization, cell problem, high contrast, continuum of scales

AMS subject classifications. 34E13, 35B27

DOI. 10.1137/100813968

1. Introduction.

Consider the partial differential equation

$$\begin{cases} -\mathrm{div}(a(x)\nabla u(x)) = g(x), \quad x \in \Omega, g \in L^2(\Omega), \quad a(x) = \{a_{ij} \in L^\infty(\Omega)\} \\ u = 0 \quad \text{on } \partial\Omega, \end{cases} \tag{1.1}$$

where Ω is a bounded subset of $\mathbb{R}^d$ with a smooth boundary (e.g., C^2) and a is symmetric and uniformly elliptic on Ω. It follows that the eigenvalues of a are uniformly bounded from below and above by two strictly positive constants, denoted by $\lambda_{\min}(a)$ and $\lambda_{\max}(a)$. Precisely, for all $\xi \in \mathbb{R}^d$ and $x \in \Omega$,

$$\lambda_{\min}(a)|\xi|^2 \leq \xi^T a(x)\xi \leq \lambda_{\max}(a)|\xi|^2. \tag{1.2}$$

In this paper, we are interested in the homogenization of (1.1) (and its parabolic and hyperbolic analogues in sections 4 and 5), but not in the classical sense, i.e., that of asymptotic analysis [9] or that of G or H-convergence (see [47], [57], [32]) in which one considers a sequence of operators $-\mathrm{div}(a_\epsilon \nabla)$ and seeks to characterize limits of solution. We are interested in the homogenization of (1.1) in the sense of "numerical homogenization," i.e., that of the approximation of the solution space of (1.1) by a finite-dimensional space.

This approximation is not based on concepts of scale-separation and/or of ergodicity but on compactness properties, i.e., the fact that the unit ball of the solution space is

*Received by the editors November 8, 2010; accepted for publication (in revised form) August 3, 2011; published electronically November 1, 2011.

http://www.siam.org/journals/mms/9-4/81396.html

†Computing & Mathematical Sciences, California Institute of Technology, MC 217-50 Pasadena, CA 91125 (owhadi@caltech.edu). The work of this author was partially supported by the National Science Foundation under award CMMI-092600 and the Department of Energy National Nuclear Security Administration under award DE-FC52-08NA28613.

‡Mathematical Institute, University of Oxford, Oxford, OX1 3LB, United Kingdom (zhange@maths.ox.ac.uk). The work of this author was partially supported by the EPSRC Science and Innovation award to the Oxford Centre for Nonlinear PDE (EP/E035027/1).

compactly embedded into $H_0^1(\Omega)$ if source terms (g) are integrable enough. This higher integrability condition on g is necessary because if g spans $H^{-1}(\Omega)$, then the solution space of (1.1) is $H_0^1(\Omega)$ (and it is not possible to obtain a finite-dimensional approximation subspace of $H_0^1(\Omega)$ with arbitrary accuracy in the H^1-norm). However, if g spans the unit ball of $L^2(\Omega)$, then the solution space of (1.1) shrinks to a compact subset of $H_0^1(\Omega)$ that can be approximated to an arbitrary accuracy in the H^1-norm by finite-dimensional spaces [10] (observe that if $a = I_d$, then the solution space is a closed bounded subset of $H^2 \cap H_0^1(\Omega)$, which is known to be compactly embedded into $H_0^1(\Omega)$).

The identification of localized bases spanning accurate approximation spaces relies on a transfer property obtained in [10]. For the sake of completeness, we will give a short reminder of that property in section 2. In section 3, we will construct localized approximation bases with rigorous error estimates (under no further assumptions on a than those given above). In subsection 3.4, we will also address the high-contrast scenario in which $\lambda_{\max}(a)$ is allowed to be large. In sections 4 and 5, we will show that the approximation spaces obtained by solving localized elliptic PDEs remain accurate for parabolic and hyperbolic time-dependent problems. We refer the reader to section 6 for numerical experiments. We refer the reader to Appendix B for further discussion and a proof of the strong compactness of the solution space when the range of g is a closed bounded subset of $H^{-\nu}(\Omega)$ with $\nu < 1$ (this notion of strong compactness constitutes a simple but fundamental link between classical homogenization, numerical homogenization, and reduced order modeling).

2. A reminder on the flux-norm and the transfer property. Recall that the key element in G and H convergence is a notion of "compactness by compensation" combined with convergence of fluxes. Here, the notion of compactness is combined with a flux-norm introduced in [10].

The flux-norm. We will now give a short reminder on the flux-norm and its properties.

DEFINITION 2.1. *For $k \in (L^2(\Omega))^d$, denote by k_{pot} the potential portion of the Weyl–Helmholtz decomposition of k. Recall that k_{pot} is the orthogonal projection of k onto $\{\nabla f : f \in H_0^1(\Omega)\}$ in $(L^2(\Omega))^d$.*

DEFINITION 2.2. *For $\psi \in H_0^1(\Omega)$, define*

$$\|\psi\|_{a\text{-flux}} \coloneqq \|(a\nabla\psi)_{\text{pot}}\|_{(L^2(\Omega))^d}. \tag{2.1}$$

We call $\|\psi\|_{a\text{-flux}}$ the flux-norm of Ψ.

The following proposition shows that the flux-norm is equivalent to the energy norm if $\lambda_{\min}(a) > 0$ and $\lambda_{\min}(a) < \infty$.

PROPOSITION 2.1 (see [10, Proposition 2.1]). *$\|.\|_{a\text{-flux}}$ is a norm on $H_0^1(\Omega)$. Furthermore, for all $\psi \in H_0^1(\Omega)$,*

$$\lambda_{\min}(a)\|\nabla\psi\|_{(L^2(\Omega))^d} \leq \|\psi\|_{a\text{-flux}} \leq \lambda_{\max}(a)\|\nabla\psi\|_{(L^2(\Omega))^d}. \tag{2.2}$$

Motivations behind the flux-norm. There are three main motivations behind the introduction of the flux-norm.

- The flux-norm allows us to obtain approximation error estimates independent from both the minimum and maximum eigenvalues of a. In fact, the flux-norm of the solution of (1.1) is independent from a altogether since

$$\|u\|_{a\text{-flux}} = \|\nabla\Delta^{-1}g\|_{(L^2(\Omega))^d}. \tag{2.3}$$

- The $(\cdot)_{\text{pot}}$ in the a-flux-norm is explained by the fact that in practice, we are interested in fluxes (of heat, stress, oil, pollutant) entering or exiting a given domain. Furthermore, for a vector field ξ, $\int_{\partial\Omega}\xi\cdot n\mathrm{d}s=\int_{\Omega}\mathrm{div}(\xi_{\text{pot}})\mathrm{d}x$, which means that the flux entering or exiting is determined by the potential part of the vector field.
- Classical homogenization is associated with two types of convergence: convergence of energies (Γ-convergence [33], [15]) and convergence of fluxes (G- or H-convergence [47], [32], [58], [57], [46]). Similarly, one can define an energy norm and a flux-norm.

The transfer property. For V, a finite-dimensional linear subspace of $H^1_0(\Omega)$, we define

$$(\mathrm{div}\, a\nabla V) \coloneqq \mathrm{span}\{\mathrm{div}(a\nabla v)\colon v\in V\}. \tag{2.4}$$

Note that $(\mathrm{div}\, a\nabla V)$ is a finite-dimensional subspace of $H^{-1}(\Omega)$.

THEOREM 2.1 (transfer property of the flux-norm; see [10, Theorem 2.1]). *Let V' and V be finite-dimensional subspaces of $H^1_0(\Omega)$. For $f\in L^2(\Omega)$, let u be the solution of* (1.1) *with conductivity a, and let u' be the solution of* (1.1) *with conductivity a'. If* $(\mathrm{div}\, a\nabla V)=(\mathrm{div}\, a'\nabla V')$, *then*

$$\inf_{v\in V}\frac{\|u-v\|_{a\text{-flux}}}{\|g\|_{L^2(\Omega)}}=\inf_{v\in V'}\frac{\|u'-v\|_{a'\text{-flux}}}{\|g\|_{L^2(\Omega)}}. \tag{2.5}$$

The usefulness of (2.5) can be illustrated by considering $a'=I$ so that $\mathrm{div}\, a'\nabla=\Delta$. Then, $u'\in H^2$, and therefore V' can be chosen as, e.g., the standard piecewise linear finite element method space, on a regular triangulation of Ω of resolution h, with nodal basis $\{\phi_i\}$. The space V is then defined by its basis $\{\theta_i\}$ determined by

$$\begin{cases}\mathrm{div}(a\nabla\theta_i)=\Delta\phi_i & \text{in } \Omega,\\ \theta_i=0 & \text{on } \partial\Omega.\end{cases} \tag{2.6}$$

Equation (2.5) shows that the approximation error estimate associated with the space V and the problem with arbitrarily rough coefficients is (in the a-flux-norm) equal to the approximation error estimate associated with piecewise linear elements and the space $H^2(\Omega)$. More precisely,

$$\sup_{g\in L^2(\Omega)}\inf_{v\in V}\frac{\|u-v\|_{a\text{-flux}}}{\|g\|_{L^2(\Omega)}}\leq Ch, \tag{2.7}$$

where C does not depend on a.

We refer the reader to [22], [25], and [11] for recent results on finite element methods for high-contrast ($\lambda_{\max}(a)/\lambda_{\min}(a)>>1$) but nondegenerate ($\lambda_{\min}(a)=\mathcal{O}(1)$) media under specific assumptions on the morphology of the (high-contrast) inclusions (in [22], the mesh has to be adapted to the morphology of the inclusions). Observe that the proposed method remains accurate if the medium is both of high contrast and degenerate ($\lambda_{\min}(a)<<1$), without any further limitations on a, at the cost of solving PDEs (2.6) over the whole domain Ω.

Remark 2.1. We refer the reader to [10] for the optimal constant C in (2.7). This question of optimal approximation with respect to a linear finite-dimensional space is related to the Kolmogorov n-width [54], [44], which measures how accurately a given set of functions can be approximated by linear spaces of dimension n in a given norm.

A surprising result of the theory of n-widths is the nonuniqueness of the space realizing the optimal approximation [54]. Observe also that, as another consequence of the transfer property (2.5), a h^{k+1} rate of convergence can be achieved in (2.7) by replacing $\boldsymbol{\phi}_i$ with higher-order basis functions in (2.6), and $\|g\|_{L^2}$ with $\|g\|_{H^k}$ in (2.7). Similarly, an exponential rate of convergence can be achieved if the source terms g are analytic. This is the reason behind the nearly exponential rate of convergence observed in [6] for harmonic functions (i.e., with zero source terms, and particular "buffer" solutions computed near the boundary) and bounded (nonhigh) contrast media.

3. Localization of the transfer property. The elliptic PDEs (2.6) have to be solved on the whole domain $\boldsymbol{\Omega}$. Is it possible to localize the computation of the basis elements $\boldsymbol{\theta}_i$ to a neighborhood of the support of the elements $\boldsymbol{\phi}_i$? Observe that the support of each $\boldsymbol{\phi}_i$ is contained in a ball $B(x_i, Ch)$ of center x_i (the node of the coarse mesh associated with x_i) of radius Ch. Let $0 < \boldsymbol{\alpha} \leq 1$. Solving the PDEs (2.6) on subdomains of $\boldsymbol{\Omega}$ (containing the support of $\boldsymbol{\phi}_i$) may, a priori, increase the error estimate in the right-hand side of (2.5). This increase can, in fact, be linked to the decay of the Green's function of the operator $-\mathrm{div}(a\nabla)$. The slower the decay, the larger the degradation of those approximation error estimates. Inspired by the strategy used in [35] for controlling cell resonance errors in the computation of the effective conductivity of periodic or stochastic homogenization (see also [36], [53], [63]), we will replace the operator $-\mathrm{div}(a\nabla)$ with the operator $\frac{1}{T} - \mathrm{div}(a\nabla)$ in the left-hand side of (2.6) in order to artificially introduce an exponential decay in the Green's function. A fine-tuning of T is required, because although a decrease in T improves the decay of the Green's function, it also deteriorates the accuracy of the transfer property. In order to limit this deterioration, we will transfer a vector space with a higher approximation order than the one associated with piecewise linear elements. Let us now give the main result.

3.1. Localized basis functions. Let $h \in (0, 1)$. Let X_h be an approximation subvector space of $H^1_0(\boldsymbol{\Omega})$ such that the following are true.

- X_h is spanned by basis functions $(\boldsymbol{\varphi}_i)_{1 \leq i \leq N}$ (with $N = \mathcal{O}(|\boldsymbol{\Omega}|/h^d)$) with supports in $B(x_i, Ch)$, where the x_i are the nodes of a regular triangulation of $\boldsymbol{\Omega}$ of resolution h.
- X_h satisfies the following approximation properties: For all $f \in H^1_0(\boldsymbol{\Omega}) \cap H^2(\boldsymbol{\Omega})$,

$$\inf_{v \in X_h} \|f - v\|_{H^1_0(\boldsymbol{\Omega})} \leq Ch \|f\|_{H^2(\boldsymbol{\Omega})}, \tag{3.1}$$

and for all $f \in H^1_0(\boldsymbol{\Omega}) \cap H^3(\boldsymbol{\Omega})$,

$$\inf_{v \in X_h} \|f - v\|_{H^1_0(\boldsymbol{\Omega})} \leq Ch^2 \|f\|_{H^3(\boldsymbol{\Omega})}. \tag{3.2}$$

- For all i,

$$\int_{\boldsymbol{\Omega}} |\nabla \boldsymbol{\varphi}_i|^2 \leq Ch^{d-2}. \tag{3.3}$$

- For all coefficients c_i,

$$h^d \sum_i c_i^2 \leq C \left\| \sum_i c_i \nabla \boldsymbol{\varphi}_i \right\|^2_{L^2(\boldsymbol{\Omega})}. \tag{3.4}$$

Remark 3.1. Examples of such spaces can be found in [17] and constructed using piecewise quadratic polynomials. From the first bullet point it follows that h can be thought of as the diameter of the support of the elements φ_i. The largest parameter h^d/C satisfying (3.4) is the minimal eigenvalue of the stiffness matrix $(\int_\Omega (\nabla\varphi_i)^T \nabla\varphi_j)_{1\le i,j\le N}$, and condition (3.4) is obtained from the regularity of the tessellation of Ω. In fact, the proof of Proposition 3.2 shows that condition (3.4) can be relaxed to the assumption of existence of a constant $d_\varphi > 0$ independent from h such that for all coefficients c_i,

$$h^{d_\varphi} \sum_i c_i^2 \le C \left\| \sum_i c_i \nabla\varphi_i \right\|^2_{L^2(\Omega)}. \tag{3.5}$$

Throughout this paper, we will write C for any constant that does not depend on h (but may depend on d, Ω, and the essential supremum and infimum of the maximum and minimum eigenvalues of a over Ω). Let $\alpha \in (0,1)$ and $C_1 > 0$. For each basis element φ_i of X_h, let ψ_i be the solution of

$$\begin{cases} h^{-2\alpha}\psi_i - \operatorname{div}(a\nabla\psi_i) = \Delta\varphi_i & \text{in } B\Big(x_i, C_1 h^\alpha \ln \tfrac{1}{h}\Big) \cap \Omega, \\ \psi_i = 0 & \text{on } \partial\Big(B\Big(x_i, C_1 h^\alpha \ln \tfrac{1}{h}\Big) \cap \Omega\Big). \end{cases} \tag{3.6}$$

Let

$$V_h := \operatorname{span}(\psi_i) \tag{3.7}$$

be the linear space spanned by the elements ψ_i.

THEOREM 3.1. *For $g \in L^2(\Omega)$, let u be the solution of* (1.1) *in $H_0^1(\Omega)$ and u_h the solution of* (1.1) *in V_h. There exists $C_0 > 0$ such that for $C_1 \ge C_0$, we have*

$$\frac{\|u - u_h\|_{H_0^1(\Omega)}}{\|g\|_{L^2(\Omega)}} \le \begin{cases} Ch & \text{if } \alpha \in \Big(0, \tfrac{1}{2}\Big], \\ Ch^{2-2\alpha} & \text{if } \alpha \in \Big[\tfrac{1}{2}, 1\Big), \end{cases} \tag{3.8}$$

where the constants C and C_0 depend on a, d, and Ω but not on h.

Remark 3.2. Theorem 3.1 shows that the convergence rate in the approximation error remains optimal (i.e., proportional to h) after localization if $0 < \alpha \le 1/2$ and decays to 0 as $h^{2-2\alpha}$ for $\frac{1}{2} \le \alpha < 1$. In particular, choosing localized domains with radii $\mathcal{O}(\sqrt{h} \ln \frac{1}{h})$ is sufficient to obtain the optimal convergence rate $\mathcal{O}(h)$. Observe that the choice of the constant α in (3.6) is arbitrary.

Remark 3.3. According to Theorem 3.1, the constant C_1 in (3.6) needs to be chosen larger than C_0 to achieve the convergence rate $h + h^{2-2\alpha}$. The constant C_0 depends on α, d, $\lambda_{\min}(a)$, and $\lambda_{\max}(a)$. The constant C in the right-hand side of (3.8) also depends on α, d, $\lambda_{\min}(a)$, and $\lambda_{\max}(a)$. It is possible to give an explicit value for C_0 and C by tracking constants in the proof (in particular, as stated in subsection 3.4, the dependence on $\lambda_{\max}(a)$ can be removed if the elements Ψ_i are computed on subdomains with added buffer zones around high-conductivity inclusions).

Remark 3.4. If one uses piecewise linear basis elements instead of the elements φ_i (i.e., in the absence of property (3.2)), then the estimate in the right-hand side of (3.8) deteriorates to $h^{1-2\alpha}$. The proof of this remark is similar to that of Theorem 3.1. The main modification lies in replacing h^2/T by h/T in (3.10) and (3.16).

Remark 3.5. One could use piecewise linear basis elements instead of the elements φ_i, and also remove the term $h^{-2\alpha}\psi_i$ from the transfer property (3.6). In this situation, we numerically observe a rate of convergence of h for periodic, stochastic, and low-contrast media after localization of (3.6) to balls of radii $\mathcal{O}(h)$. In these *particular* situations (characterized by short range correlations in a), the term $h^{-2\alpha}\psi_i$ should be avoided to obtain the optimal convergence rate h after localization to subdomains of size $\mathcal{O}(h)$. In that sense, the estimate in the right-hand side of (3.8) corresponds to a *worst case scenario* with respect to the medium a (characterized by long range correlations), requiring the introduction of the term $h^{-1}\psi_i$ and a localization to subdomains of size $\mathcal{O}(\sqrt{h}\ \ln\ \frac{1}{h})$ for the optimal convergence rate h.

Remark 3.6. For the elliptic problem, computational gains result from localization (the elements ψ_i are computed on subdomains $\mathbf{\Omega}_i$ of $\mathbf{\Omega}$), parallelization (the elements ψ_i can be computed independently from each other), and the fact that the same basis can be used for different right-hand sides g in (1.1). Computational gains are even more significant for time-dependent problems because, once an accurate basis has been determined for the elliptic problem, the same basis can be used for the associated (parabolic and hyperbolic) time-dependent problems with the same accuracy (we refer the reader to sections 4 and 5). For the wave equation with rough bulk modulus and density coefficients, the proposed method (based on precomputing basis elements as solutions of localized elliptic PDEs) remains accurate, provided that high frequencies are not strongly excited ($\partial_t g \in L^2$).

On localization. We refer the reader to [22], [25], and [6] for recent localization results for divergence-form elliptic PDEs. The strategy of [22] is to construct triangulations and finite element bases that are adapted to the shape of high-conductivity inclusions via coefficient dependent boundary conditions for the subgrid problems (assuming a to be piecewise constant and the number of inclusions bounded). The strategy of [25] is to solve local eigenvalue problems, observing that only a few eigenvectors are sufficient to obtain a good preconditioner. Both [22] and [25] require specific assumptions on the morphology and number of inclusions. The idea of the strategy is to observe that if a is piecewise constant and the number of inclusions bounded, then u is locally H^2 away from the interfaces of the inclusions. The inclusions can then be taken care of by adapting the mesh and the boundary values of localized problems or by observing that those inclusions will affect only a finite number of eigenvectors.

The strategy of [6] is to construct generalized finite elements by partitioning the computational domain into to a collection of preselected subsets and compute optimal local bases (using the concept of n-widths [55]) for the approximation of harmonic functions. Local bases are constructed by solving local eigenvalue problems (corresponding to computing eigenvectors of P^*P, where P is the restriction of a-harmonic functions from ω^* onto $\omega \subset \omega^*$, P^* is the adjoint of P, and ω is a subdomain of $\mathbf{\Omega}$ surrounded by a larger subdomain ω^*). The method proposed in [6] achieves a nearly exponential convergence rate (in the number of precomputed basis functions) for harmonic functions. Nonzero right-hand sides (g) are then taken care of by solving (for each different g) particular solutions on preselected subsets with a constant Neumann boundary condition (determined according to the consistency condition).

As explained in Remark 2.1, the nearly exponential rate of convergence observed in [6] is explained by the fact that the source space considered in [6] is more regular than L^2 (since [6] requires the computation particular (local) solutions for each right-hand side g and each nonzero boundary condition, the basis obtained in [6] is in fact adapted to a-harmonic functions away from the boundary). The strategy proposed here can also be

used to achieve exponential convergence for analytic source terms g by employing higher-order basis functions φ_i in (3.6). Furthermore, as shown in sections 4, 5, and 3.4, the method proposed here allows for the numerical homogenization of time-dependent problems (because it does not require the computation of particular solutions for different source or boundary terms) and can be extended to high-contrast media. We also note that the basis functions ψ_i are simpler and cheaper to compute (see (3.6)) than the eigenvectors of P^*P required by [6]. We refer the reader to p. 16 of [6] for a discussion on the cost of this added complexity.

3.2. On numerical homogenization. By now, the field of numerical homogenization has become large enough that it is not possible to give an exhaustive review in this short paper. Therefore, we will restrict our attention to works directly related to our work.

- The multiscale finite element method [40], [62], [41] can be seen as a numerical generalization of this idea of oscillating test functions found in H-convergence. A convergence analysis for periodic media revealed a resonance error introduced by the microscopic boundary condition [40], [41]. An oversampling technique was proposed to reduce the resonance error [40].
- Harmonic coordinates play an important role in various homogenization approaches, both theoretical and numerical. These coordinates were introduced in [42] in the context of random homogenization. Next, harmonic coordinates have been used in one-dimensional and quasi-one-dimensional divergence-form elliptic problems [7], [5], allowing for efficient finite-dimensional approximations. The connection of these coordinates with classical homogenization is made explicit in [2] in the context of multiscale finite element methods. The idea of using particular solutions in numerical homogenization to approximate the solution space of (1.1) appears to have been first proposed in reservoir modeling in the 1980s [16], [61] (in which a global scale-up method was introduced based on generic flow solutions, i.e., flows calculated from generic boundary conditions). Its rigorous mathematical analysis was done only recently [49] and is based on the fact that solutions are in fact H^2-regular with respect to harmonic coordinates (recall that they are H^1-regular with respect to Euclidean coordinates). The main message here is that if the right-hand side of (1.1) is in L^2, then solutions can be approximated at small scales (in the H^1-norm) by linear combinations of d (linearly independent) particular solutions (d being the dimension of the space). In that sense, harmonic coordinates are only good candidates for being d linearly independent particular solutions.
  The idea of a global change of coordinates analogous to harmonic coordinates has been implemented numerically in order to up-scale porous media flows [27], [26], [16]. We refer the reader, in particular, to a recent review article [16] for an overview of some main challenges in reservoir modeling and a description of global scale-up strategies based on generic flows.
- In [24], [29], the structure of the medium is numerically decomposed into a microscale and a macroscale (meso-scale), and solutions of cell problems are computed on the microscale, providing local homogenized matrices that are transferred (upscaled) to the macroscale grid. This procedure allows one to obtain rigorous homogenization results with controlled error estimates for nonperiodic media of the form $a(x, \frac{x}{\epsilon})$ (where $a(x, y)$ is assumed to be smooth in x and periodic or ergodic with specific mixing properties in y). Moreover, it is shown that the numerical algorithms associated with heterogeneous multiscale

methods (HMM) and multiscale finite element methods (MsFEM) can be implemented for a class of coefficients that is much broader than $a(x,\frac{x}{\epsilon})$. We refer the reader to [34] for convergence results on the heterogeneous multiscale method in the framework of G- and Γ-convergence.

- More recent work includes an adaptive projection based method [48], which is consistent with homogenization when there is scale-separation, leading to adaptive algorithms for solving problems with no clear scale-separation, fast and sparse chaos approximations of elliptic problems with stochastic coefficients [60], [37], [23], finite-difference approximations of fully nonlinear, uniformly elliptic PDEs with Lipschitz continuous viscosity solutions [19], and operator splitting methods [4], [3].
- We refer the reader to [13], [12] (and the references therein) for the most recent results on homogenization of scalar divergence-form elliptic operators with stochastic coefficients. Here, the stochastic coefficients $a(x/\varepsilon,\omega)$ are obtained from stochastic deformations (using random diffeomorphisms) of the periodic and stationary ergodic setting.

3.3. Proof of Theorem 3.1. For each basis element φ_i of X_h, let $\psi_{i,T}$ be the solution of

$$\begin{cases} \frac{1}{T}\psi_{i,T} - \operatorname{div}(a\nabla\psi_{i,T}) = \Delta\varphi_i & \text{in } \Omega, \\ \psi_{i,T} = 0 & \text{on } \partial\Omega. \end{cases} \tag{3.9}$$

The following proposition will allow us to control the impact of the introduction of the term $\frac{1}{T}$ in the transfer property. Observe that the domain of PDE (3.9) is still Ω (our next step will be to localize it to $\Omega_i \subset \Omega$).

PROPOSITION 3.1. *For $g \in L^2(\Omega)$, let u be the solution of (1.1) in $H_0^1(\Omega)$. Then, there exists $v \in \operatorname{span}(\psi_{i,T})$ such that*

$$\frac{\|u-v\|_{H_0^1(\Omega)}}{\|g\|_{L^2(\Omega)}} \leq C\left(h + \frac{h^2}{T}\right). \tag{3.10}$$

Furthermore, writing $v \coloneqq \sum_i c_i\psi_{i,T}$, we have

$$\sum_i c_i^2 \leq Ch^{-d}(1+T^{-2})\|g\|^2_{L^2(\Omega)}. \tag{3.11}$$

Proof. Let $v = \sum_i c_i\psi_{i,T}$. We have

$$\frac{u-v}{T} - \operatorname{div}(a\nabla(u-v)) = g + \frac{u}{T} - \sum_i c_i\Delta\varphi_i. \tag{3.12}$$

Define $a[v]$ to be the energy norm $a[v] \coloneqq \int_\Omega (\nabla v)^T a\nabla v$. Multiplying (3.12) by $u-v$ and integrating by parts, we obtain that

$$\frac{\|u-v\|^2_{L^2(\Omega)}}{T} + a[u-v] = \int_\Omega (u-v)\left(g + \frac{u}{T} - \sum_i c_i\Delta\varphi_i\right). \tag{3.13}$$

Write $c_i = c_{i,1} + c_{i,2}$ and let w_1 and w_2 be the solutions of $\Delta w_1 = g - \sum_i c_{i,1}\Delta\varphi_i$ and $\Delta w_2 = \frac{u}{T} - \sum_i c_{i,2}\Delta\varphi_i$ with Dirichlet boundary conditions on $\partial\Omega$. Then, we obtain by integration by parts and the Cauchy–Schwarz inequality that

$$\frac{\|u-v\|^2_{L^2(\Omega)}}{T} + a[u-v] \leq \|\nabla(u-v)\|_{(L^2(\Omega))^d}(\|\nabla w_1\|_{(L^2(\Omega))^d} + \|\nabla w_2\|_{(L^2(\Omega))^d}). \tag{3.14}$$

Using (3.1), we can choose $(c_{i,1})$ so that

$$\|\nabla w_1\|_{(L^2(\Omega))^d} \leq Ch\|g\|_{L^2(\Omega)}. \tag{3.15}$$

Using (3.2), we can choose $(c_{i,2})$ so that

$$\|\nabla w_2\|_{(L^2(\Omega))^d} \leq C\frac{h^2}{T}\|u\|_{H^1_0(\Omega)}; \tag{3.16}$$

we conclude the proof of the approximation (3.10) by observing that $\|u\|_{H^1_0(\Omega)} \leq C\|g\|_{L^2(\Omega)}$. Let us now prove (3.11). First, observe that (3.4) and the triangular inequality imply that

$$\left(\sum_i (c_i)^2\right)^{\frac{1}{2}} \leq Ch^{-\frac{d}{2}}\left(\left\|\sum_i c_{i,1}\nabla\varphi_i\right\|_{L^2(\Omega)} + \left\|\sum_i c_{i,2}\nabla\varphi_i\right\|_{L^2(\Omega)}\right). \tag{3.17}$$

Next, we obtain from (3.15) and Poincaré inequality that

$$\left\|\sum_i c_{i,1}\nabla\varphi_i\right\|_{L^2(\Omega)} \leq C\|g\|_{L^2(\Omega)} \tag{3.18}$$

and

$$\left\|\sum_i c_{i,2}\nabla\varphi_i\right\|_{L^2(\Omega)} \leq C\frac{1}{T}\|g\|_{L^2(\Omega)}. \tag{3.19}$$

We conclude by combining (3.18) and (3.19) with (3.17). ∎

We will now control the error induced by the localization of the elliptic problem (3.9). To this end, for each basis element φ_i of X_h, write S_i for the intersection of the support of φ_i with Ω and let Ω_i be a subset of Ω containing S_i such that $\operatorname{dist}(S_i, \Omega/\Omega_i) > 0$. Let also ψ_{i,T,Ω_i} be the solution of

$$\begin{cases} \frac{1}{T}\psi_{i,T,\Omega_i} - \operatorname{div}(a\nabla\psi_{i,T,\Omega_i}) = \Delta\varphi_i & \text{in } \Omega_i, \\ \psi_{i,T,\Omega_i} = 0 & \text{on } \partial\Omega_i. \end{cases} \tag{3.20}$$

For $A, B \subset \Omega$, write $d(A,B)$ for the Euclidean distance between the sets A and B.

Proposition 3.2. *Extending ψ_{i,T,Ω_i} by 0 on Ω/Ω_i, we have*

$$\|\psi_{i,T} - \psi_{i,T,\Omega_i}\|_{H^1(\Omega)} \leq \frac{Ch^{\frac{d}{2}-1}(T^{-1}+1)}{(\operatorname{dist}(S_i, \Omega/\Omega_i))^{d+1}}\ \exp\left(-\frac{\operatorname{dist}(S_i, \Omega/\Omega_i)}{C\sqrt{T}}\right). \tag{3.21}$$

We refer the reader to Appendix A for the proof of Proposition 3.2.

Taking $\Omega_i := B(x_i, C_1 h^\alpha \ln \frac{1}{h}) \cap \Omega$ (we use the particular notation C_1 because our proof of accuracy requires the specific constant to be large enough, i.e., larger than a constant depending on the parameter C appearing in the right-hand side of (3.21) and the parameter C describing the balls $B(x_i, Ch)$ containing the support of the basis functions $(\varphi_i)_{1\leq i\leq N}$ introduced in subsection 3.1) and $T = h^{2\alpha}$ in (3.21) of Proposition 3.2, we obtain for C_1 large enough (but independent from h) that

$$\|\psi_{i,T} - \psi_{i,T,\Omega_i}\|_{H^1(\Omega)} \leq Ch^{d+1+2\alpha}. \tag{3.22}$$

Let u be the solution of (1.1) in $H_0^1(\Omega)$. Using Proposition 3.1, we obtain that there exist coefficients c_i such that

$$\left\| u - \sum_i c_i \psi_{i,T} \right\|_{H_0^1(\Omega)} \leq C(h + h^{2-2\alpha}) \|g\|_{L^2(\Omega)} \tag{3.23}$$

and

$$\sum_i c_i^2 \leq Ch^{-d-4\alpha} \|g\|_{L^2(\Omega)}^2. \tag{3.24}$$

Using the triangle inequality, it follows that

$$\left\| u - \sum_i c_i \psi_{i,T,\Omega_i} \right\|_{H_0^1(\Omega)} \leq C(h + h^{2-2\alpha}) \|g\|_{L^2(\Omega)} + \sum_i |c_i| \|\psi_{i,T} - \psi_{i,T,\Omega_i}\|_{H^1(\Omega)}, \tag{3.25}$$

whence, from the Cauchy–Schwarz inequality,

$$\begin{aligned} \left\| u - \sum_i c_i \psi_{i,T,\Omega_i} \right\|_{H_0^1(\Omega)} &\leq C(h + h^{2-2\alpha}) \|g\|_{L^2(\Omega)} \\ &\quad + \left(\sum_i |c_i|^2 \right)^{\frac{1}{2}} \left(\sum_i \|\psi_{i,T} - \psi_{i,T,\Omega_i}\|_{H^1(\Omega)}^2 \right)^{\frac{1}{2}}. \end{aligned} \tag{3.26}$$

Combining (3.26) with (3.24), we obtain that

$$\begin{aligned} \left\| u - \sum_i c_i \psi_{i,T,\Omega_i} \right\|_{H_0^1(\Omega)} &\leq C(h + h^{2-2\alpha}) \|g\|_{L^2(\Omega)} \\ &\quad + Ch^{-\frac{d}{2}-2\alpha} \|g\|_{L^2(\Omega)} \left(\sum_i \|\psi_{i,T} - \psi_{i,T,\Omega_i}\|_{H^1(\Omega)}^2 \right)^{\frac{1}{2}}. \end{aligned} \tag{3.27}$$

Using (3.22) in (3.27), we obtain that

$$\left\| u - \sum_i c_i \psi_{i,T,\Omega_i} \right\|_{H_0^1(\Omega)} \leq C(h + h^{2-2\alpha}) \|g\|_{L^2(\Omega)}. \tag{3.28}$$

Observe that it is the exponential decay in (3.21) that allows us to compensate for the large term on the right-hand side of (3.27) via (3.22). This concludes the proof of Theorem 3.1.

3.4. On localization with high contrast. The constant C in the approximation error estimate (3.8) depends, a priori, on the contrast of a. Is it possible to localize the computation of bases for V_h when the contrast of a is high? The purpose of this subsection is to show that the answer is "yes," provided that there is a buffer zone between the boundaries of localization subdomains and the supports of the elements φ_i, where the contrast of a remains bounded. More precisely, assume that Ω is the disjoint union of Ω_{bounded} and Ω_{high}. Assume that (1.2) holds only on Ω_{bounded}, and that on Ω_{high} we have

$$\lambda_{\min}(a)|\xi|^2 \leq \xi^T a(x)\xi \leq \gamma|\xi|^2, \tag{3.29}$$

where γ can be arbitrarily large. Practical examples include media characterized by a bounded contrast background with high-conductivity inclusions or channels. Let ψ_i^{high} be the solution of

$$\begin{cases} h^{-2\alpha}\psi_i^{\text{high}} - \operatorname{div}(a\nabla\psi_i^{\text{high}}) = \Delta\varphi_i & \text{in } \Omega_i, \\ \psi_i = 0 & \text{on } \partial\Omega_i. \end{cases} \tag{3.30}$$

Let

$$V_h^{\text{high}} := \operatorname{span}(\psi_i^{\text{high}}) \tag{3.31}$$

be the linear space spanned by the elements ψ_i^{high}. For each i, define b_i to be the largest number r such that there exists a subset Ω_i' such that the closure of Ω_i' contains the support of φ_i, $(\Omega_i')^r$ is a subset of Ω_i (where A^r are the set of points of Ω that are at distance at most r for A), and $(\Omega_i')^r/\Omega_i'$ is a subset of Ω_{bounded}. If no such subset exists, we set $b_i := 0$. b_i can be interpreted as the non–high-contrast buffer distance between the support of φ_i and the boundary of Ω_i. We refer the reader to Figure 3.1 for illustrations of the buffer distance.

THEOREM 3.2. *For $g \in L^2(\Omega)$, let u be the solution of (1.1) in $H_0^1(\Omega)$ and u_h the solution of (1.1) in V_h^{high}. There exists $C_0 > 0$ such that if for all i, $b_i \geq C_0 h^\alpha \ln \frac{1}{h}$, then*

$$\frac{\|u - u_h\|_{H_0^1(\Omega)}}{\|g\|_{L^2(\Omega)}} \leq \begin{cases} Ch & \text{if } \alpha \in \left(0, \frac{1}{2}\right], \\ Ch^{2-2\alpha} & \text{if } \alpha \in \left[\frac{1}{2}, 1\right), \end{cases} \tag{3.32}$$

where the constants C and C_0 depend on $\lambda_{\min}(a)$, $\lambda_{\max}(a)$ (the bounds on a in Ω_{bounded}), d, and Ω but not on h and γ (γ is the upper bound on a on Ω_{high}).

Remark 3.7. Recall that the global basis computed in (2.6) remains accurate if the medium is both of high contrast ($\lambda_{\max}(a) >> 1$) and degenerate ($\lambda_{\min}(a) << 1$). The basis computed in (3.30) preserves the former property (of accuracy for high-contrast media) but loses the latter property (of accuracy in the degenerate case), since the constant C in (3.32) depends on $\lambda_{\min}(a)$.

Remark 3.8. Observe that local solves have to resolve the connected components of high-contrast structures. This is the price to pay for localization with high contrast in the most general case. Recall that in classical homogenization with high contrast, the limit of the homogenized operator may be a nonlocal operator (we refer the reader, for instance, to [21]). A similar phenomenon is observed here (distant points connected by

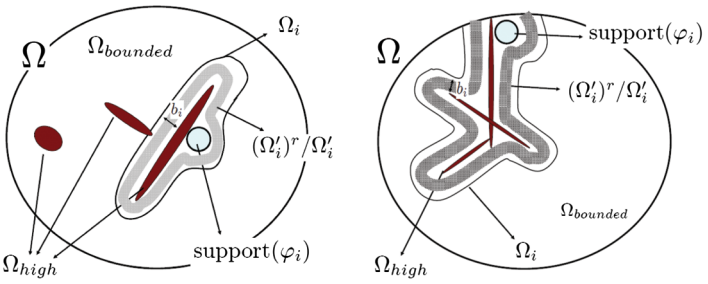

FIG. 3.1. *Illustrations of the buffer distance.*

high-conductivity channels are associated with a low resistance metric and a large coupling coefficient in the numerically homogenized stiffness matrix).

The proof of Theorem 3.2 is similar to that of Theorem 3.1, but it requires a precise tracking of the constants involved. Because of the close similarity, we will not include the proof in this paper but only give its main points. First, the proof of Proposition 3.1 remains unchanged, as the constants C in (3.10) and (3.11) do not depend on the maximum eigenvalue of the conductivity a. Only the proof of Proposition 3.2 has to be adapted, and the part of the proof below Proposition 3.2 remains unchanged. This requires an application of the elements of Lemmas A.2, A.3, A.4, and A.5 to buffer subdomains $(\Omega_i')^r/\Omega_i'$. The main point is to observe that the decay of the Green's function in $(\Omega_i')^r/\Omega_i'$ can be bounded independently from γ (due to the maximum principle).

Observe that the choice of the subdomain Ω_i in (3.30) can be chosen to be the same as in (3.20) if its intersection with high-contrast inclusions is void (i.e., if the maximum eigenvalue of a over Ω_i remains bounded independently from γ); otherwise the choice of Ω_i in (3.30) has to be enlarged (when compared to that associated with (3.20)) to contain the high-contrast inclusion (plus its buffer).

4. The basis remains accurate for parabolic PDEs. The computational gain of the method proposed in this paper is particularly significant for time-dependent problems. One such problem is the parabolic equation associated with the operator $-\mathrm{div}(a\nabla)$. More precisely, consider the time-dependent PDE

$$\begin{cases} \partial_t u(x,t) - \mathrm{div}(a(x)\nabla u(x,t)) = g(x,t), \quad (x,t) \in \Omega_T; g \in L^2(\Omega_T), \\ u = 0 \quad \text{on } \partial\Omega_T, \end{cases} \tag{4.1}$$

where a and Ω satisfy the same assumptions as those associated with PDE (1.1), $\Omega_T \coloneqq \Omega \times [0,T]$ for some $T > 0$, and $\partial\Omega_T \coloneqq (\partial\Omega \times [0,T]) \cup (\Omega \times \{t = 0\})$.

Let V_h be the finite-dimensional approximation space defined in (3.7). Let u_h be the finite element solution of (4.1); i.e., u_h can be decomposed as

$$u_h(x,t) = \sum_i c_i(t)\psi_i(x) \tag{4.2}$$

and solves for all j

$$(\psi_j, \partial_t u_h)_{L^2(\Omega)} = -a[\psi_j, u_h] + (\psi_j, g)_{L^2(\Omega)} \tag{4.3}$$

with $a[v,w] \coloneqq \int_\Omega (\nabla v)^T a \nabla w$. Write

$$\|v\|^2_{L^2(0,T,H^1_0(\Omega))} \coloneqq \int_0^T \int_\Omega |\nabla v|^2(x,t)\,dx\,dt. \tag{4.4}$$

THEOREM 4.1. *We have*

$$\|(u-u_h)(.,T)\|_{L^2(\Omega)} + \|u-u_h\|_{L^2(0,T,H^1_0(\Omega))} \leq C\|g\|_{L^2(\Omega_T)}(h + h^{2-2\alpha}). \tag{4.5}$$

Proof. The proof is a generalization of the proof found in [50] (in which approximation spaces are constructed via harmonic coordinates). Let $\mathcal{A}_T$ be the bilinear form on $L^2(0,T,H^1_0(\Omega))$ defined by

$$\mathcal{A}_T[w_1,w_2] \coloneqq \int_0^T a[w_1,w_2]\,dt. \tag{4.6}$$

Observe that for all $v \in L^2(0, T, V_h)$,

$$(v, \partial_t(u - u_h))_{L^2(\Omega_T)} + \mathcal{A}_T[v, u - u_h] = 0. \tag{4.7}$$

Writing $\mathcal{A}_T[v] \coloneqq \mathcal{A}_T[v, v]$, we deduce that for $v \in L^2(0, T, V_h)$,

$$\begin{aligned} &\frac{1}{2}\|(u - u_h)(., T)\|^2_{L^2(\Omega)} + \mathcal{A}_T[u - u_h] \\ &\qquad = (u - v, \partial_t(u - u_h))_{L^2(\Omega_T)} + \mathcal{A}_T[u - v, u - u_h]. \end{aligned} \tag{4.8}$$

Using $\partial_t u_h$ in (4.3) and integrating, we obtain that

$$\|\partial_t u_h\|^2_{L^2(\Omega_T)} + \frac{1}{2}\, a[u_h(., T), u_h(., T)] = (\partial_t u_h, g)_{L^2(\Omega_T)}. \tag{4.9}$$

Using Minkowski's inequality, we deduce that

$$\|\partial_t u_h\|^2_{L^2(\Omega_T)} + a[u_h(., T), u_h(., T)] \le C\|g\|^2_{L^2(\Omega_T)}. \tag{4.10}$$

Similarly,

$$\|\partial_t u\|^2_{L^2(\Omega_T)} + a[u(., T), u(., T)] \le C\|g\|^2_{L^2(\Omega_T)}. \tag{4.11}$$

Using the Cauchy–Schwarz and Minkowski inequalities in (4.8), we obtain that

$$\|(u - u_h)(., T)\|^2_{L^2(\Omega)} + \mathcal{A}_T[u - u_h] \le C\|u - v\|_{L^2(\Omega_T)}\|g\|_{L^2(\Omega_T)} + C\mathcal{A}_T[u - v]. \tag{4.12}$$

Take $v = \mathcal{R}_h u$ to be the projection of u onto $L^2(0, T, V_h)$ with respect to the bilinear form $\mathcal{A}_T$. Observing that $-\mathrm{div}(a\nabla u) = g - \partial_t u$ with $(g - \partial_t u) \in L^2(\Omega_T)$, we obtain from Theorem 3.1 that

$$(\mathcal{A}_T[u - \mathcal{R}_h u])^{\frac{1}{2}} \le C\|g\|_{L^2(\Omega_T)}(h + h^{2-2\alpha}). \tag{4.13}$$

Let us now show (using a standard duality argument) that

$$\|u - \mathcal{R}_h u\|_{L^2(\Omega_T)} \le C(h + h^{2-2\alpha})^2\|g\|_{L^2(\Omega_T)}. \tag{4.14}$$

Choose v^* to be the solution of the following linear problem: For all $w \in L^2(0, T, H^1_0(\Omega))$,

$$\mathcal{A}_T[w, v^*] = (w, u - \mathcal{R}_h u)_{L^2(\Omega_T)}. \tag{4.15}$$

Taking $w = u - \mathcal{R}_h u$ in (4.15), we obtain that

$$\|u - \mathcal{R}_h u\|^2_{L^2(\Omega_T)} = \mathcal{A}_T[u - \mathcal{R}_h u, v^* - \mathcal{R}_h v^*]. \tag{4.16}$$

Hence by the Cauchy–Schwarz inequality and (4.13),

$$\|u - \mathcal{R}_h u\|^2_{L^2(\Omega_T)} \le C(h + h^{2-2\alpha})\|g\|_{L^2(\Omega_T)}(\mathcal{A}_T[v^* - \mathcal{R}_h v^*])^{\frac{1}{2}}. \tag{4.17}$$

Using Theorem 3.1 again, we obtain that

$$(\mathcal{A}_T[v^* - \mathcal{R}_h v^*])^{\frac{1}{2}} \leq C\|u - \mathcal{R}_h u\|_{L^2(\Omega_T)}(h + h^{2-2\alpha}). \tag{4.18}$$

Combining (4.18) with (4.17) leads to (4.14). Combining (4.12) with $v = \mathcal{R}_h u$, (4.14), and (4.13) leads to

$$\|(u - u_h)(., T)\|^2_{L^2(\Omega)} + \mathcal{A}_T[u - u_h] \leq C(h + h^{2-2\alpha})^2\|g\|^2_{L^2(\Omega_T)}, \tag{4.19}$$

which concludes the proof of Theorem 4.1. ∎

Discretization in time. Let (t_n) be a discretization of $[0, T]$ with time-steps $|t_{n+1} - t_n| = \Delta t$. Write Z^h_T, the subspace of $L^2(0, T, V_h)$, such that

$$Z^h_T = \Big\{ v \in L^2(0, T, V_h) : v(x, t) = \sum_i c_i(t)\psi_i(x),\ c_i(t) \text{ are constants on } (t_n, t_{n+1}] \Big\}. \tag{4.20}$$

Write $u_{h,\Delta t}$, the solution in Z^h_T of the following system of implicit weak formulation (such that $u_{h,\Delta t}(x, 0) \equiv 0$): For each n and $\psi \in V_h$,

$$\begin{aligned}(\psi, u_{h,\Delta t}(t_{n+1}))_{L^2(\Omega)} &= (\psi, u_{h,\Delta t}(t_n))_{L^2(\Omega)} \\ &\quad - |\Delta t| a[\psi, u_{h,\Delta t}(t_{n+1})] + \left(\psi, \int_{t_n}^{t_{n+1}} g(t)\,dt\right)_{L^2(\Omega)}.\end{aligned} \tag{4.21}$$

Then, we have the following theorem.

THEOREM 4.2. *We have*

$$\begin{aligned}&\|(u - u_{h,\Delta t})(T)\|_{L^2(\Omega)} + \|u - u_{h,\Delta t}\|_{L^2(0,T,H^1_0(\Omega))} \leq C(|\Delta t| + h + h^{2-2\alpha}) \\ &\quad \cdot (\|\partial_t g\|_{L^2(0,T,H^{-1}(\Omega))} + \|g(., 0)\|_{L^2(\Omega)} + \|g\|_{L^2(\Omega_T)}).\end{aligned} \tag{4.22}$$

The proof of Theorem 4.2 is similar to that of Theorem 1.6 of [50] and will not be given here. Observe that homogenization in space allows for a discretization in time with time-steps $\mathcal{O}(h + h^{2-2\alpha})$ without compromising the accuracy of the method.

5. The basis remains accurate for hyperbolic PDEs. Consider the hyperbolic PDE

$$\begin{cases} \rho(x)\partial_t^2 u(x, t) - \operatorname{div}(a(x)\nabla u(x, t)) = g(x, t), \quad (x, t) \in \Omega_T; g \in L^2(\Omega_T), \\ u = 0 \quad \text{on } \partial\Omega_T, \\ \partial_t u = 0 \quad \text{on } \Omega \times \{t = 0\}, \end{cases} \tag{5.1}$$

where a, Ω, Ω_T, and $\partial\Omega_T$ are defined as in section 4. In particular, a is assumed to be only uniformly elliptic and bounded ($a_{i,j} \in L^\infty(\Omega)$). We will further assume that ρ is uniformly bounded from below and above ($\rho \in L^\infty(\Omega)$ and $\operatorname{essinf} \rho(x) \geq \rho_{\min} > 0$). It is straightforward to extend the results presented here to nonzero boundary conditions (provided that frequencies larger than $1/h$ remain weakly excited, because the waves equation preserves energy, and homogenization schemes cannot recover energies put into high frequencies; see [51]). For the sake of conciseness, we will give those results with zero boundary conditions. PDE (5.1) corresponds to acoustic wave equations in a medium with density ρ and bulk modulus a^{-1}.

Let V_h be the finite-dimensional approximation space defined in (3.7). Let u_h be the finite element solution of (5.1); i.e., u_h can be decomposed as

$$u_h(x,t) = \sum_i c_i(t)\psi_i(x), \tag{5.2}$$

and solves for all j

$$(\psi_j, \partial_t^2 u_h)_{L^2(\rho,\Omega)} = -a[\psi_j, u_h] + (\psi_j, g)_{L^2(\Omega)}, \tag{5.3}$$

where

$$(v,w)_{L^2(\rho,\Omega)} \coloneqq \int_\Omega vw\rho. \tag{5.4}$$

THEOREM 5.1. *If $\partial_t g \in L^2(\Omega_T)$ and $g(x,0) \in L^2(\Omega)$, then*

$$\begin{aligned} &\|\partial_t(u-u_h)(.,T)\|_{L^2(\Omega)} + \|u-u_h\|_{L^2(0,T,H_0^1(\Omega))} \\ &\quad \le C(\|\partial_t g\|_{L^2(\Omega_T)} + \|g(x,0)\|_{L^2(\Omega)})(h+h^{2-2\alpha}). \end{aligned} \tag{5.5}$$

Remark 5.1. We refer the reader to [59] for an analysis of the suboptimal rate of convergence associated with finite-difference simulation of wave propagation in discontinuous media (see also [18], [56]). We refer the reader to [51] for an alternative upscaling strategy based on harmonic coordinates. If the medium is locally ergodic with long range correlations [8] and also characterized by scale-separation, then we refer the reader to HMM based methods [28], [1]. Homogenization based methods require that frequencies larger than $1/h$ remain weakly excited. For high frequencies, and smooth media (or away from local resonances, e.g., local, nearly resonant cavities), we refer the reader to the sweeping preconditioner method [30], [31].

Proof. Let $\mathcal{A}_T$ be the bilinear form on $L^2(0,T,H_0^1(\Omega))$ defined in (4.6). Observe that for all $v \in L^2(0,T,V_h)$,

$$(v, \partial_t^2(u-u_h))_{L^2(\rho,\Omega_T)} + \mathcal{A}_T[v, u-u_h] = 0. \tag{5.6}$$

Taking $\partial_t u - \partial_t u_h - (\partial_t u - \partial_t v)$ as a test function in (5.6) and integrating in time, we deduce that for $\partial_t v \in L^2(0,T,V_h)$,

$$\begin{aligned} &\frac{1}{2}\|\partial_t(u-u_h)(.,T)\|^2_{L^2(\rho,\Omega)} + \frac{1}{2}a[(u-u_h)(.,T)] \\ &\quad = (\partial_t(u-v), \partial_t^2(u-u_h))_{L^2(\rho,\Omega_T)} + \mathcal{A}_T[\partial_t(u-v), u-u_h], \end{aligned} \tag{5.7}$$

where $(v,w)_{L^2(\rho,\Omega_T)} \coloneqq \int_0^T \int_\Omega vw\rho\, dxdt$. Taking the derivative of the hyperbolic equation for u in time, we obtain that

$$\partial_t^3 u - \operatorname{div}(a\nabla\partial_t u) = \partial_t g. \tag{5.8}$$

Integrating (5.8) against the test function $\partial_t^2 u$ and observing that $\partial_t^2 u(x,0) = g(x,0)$, we also obtain that

$$\|\partial_t^2 u(.,T)\|^2_{L^2(\rho,\Omega)} + a[\partial_t u(.,T)] \le C(\|\partial_t g\|^2_{L^2(\Omega_T)} + \|g(x,0)\|^2_{L^2(\Omega)}). \tag{5.9}$$

Similarly, we obtain that

$$\|\partial_t^2 u_h(.,T)\|^2_{L^2(\rho,\Omega)} + a[\partial_t u_h(.,T)] \leq C(\|\partial_t g\|^2_{L^2(\Omega_T)} + \|g(x,0)\|^2_{L^2(\Omega)}). \tag{5.10}$$

Take $\partial_t v = \mathcal{R}_h \partial_t u$ to be the projection of $\partial_t u$ onto $L^2(0, T, V_h)$ with respect to the bilinear form $\mathcal{A}_T$. Observing that $-\mathrm{div}(a\nabla\partial_t u) = \partial_t g - \partial_t^2 u$ with $(g - \partial_t^2 u) \in L^2(\Omega_T)$, we obtain from (5.9) and Theorem 3.1 that

$$(\mathcal{A}_T[u - \mathcal{R}_h u])^{\frac{1}{2}} \leq C(\|\partial_t g\|_{L^2(\Omega_T)} + \|g(x,0)\|_{L^2(\Omega)})(h + h^{2-2\alpha}). \tag{5.11}$$

Furthermore, using the same duality argument as in the parabolic case, we obtain that

$$\|u - \mathcal{R}_h u\|_{L^2(\rho,\Omega_T)} \leq C(h + h^{2-2\alpha})^2(\|\partial_t g\|_{L^2(\Omega_T)} + \|g(x,0)\|_{L^2(\Omega)}). \tag{5.12}$$

Using the Cauchy–Schwarz and Minkowski inequalities and the above estimates in (5.7), we obtain that

$$\begin{aligned} &\|\partial_t(u - u_h)(.,T)\|^2_{L^2(\rho,\Omega)} + a[(u - u_h)(.,T)] \\ &\quad \leq C(h + h^{2-2\alpha})(\mathcal{A}_T[u - u_h] + \|\partial_t g\|_{L^2(\Omega_T)} + \|g(x,0)\|_{L^2(\Omega)}). \end{aligned} \tag{5.13}$$

We conclude using Grownwall's lemma. ∎

6. Numerical experiments.

6.1. Elliptic equation. We compute the solutions of (1.1) up to time 1 on the fine mesh and in the finite-dimensional approximation space V_h defined in (3.7). The physical domain is the square $[-1, 1]^2$. Global equations are solved on a fine triangulation with 66049 nodes and 131072 triangles.

The elements (φ_i) of subsection 3.1 are weighted extended B-splines (WEB) [38], [39] (obtained by tensorizing one-dimensional elements and using weight function $(1 - x^2)(1 - y^2)$ to enforce the Dirichlet boundary condition). The order of accuracy is not affected by the choice of weight function, given that the boundary is piecewise smooth. Our motivation for using WEB elements lies in the fact that, with those elements, (Dirichlet) boundary conditions become simple to enforce. This being said, any finite elements satisfying the properties (3.1), (3.2), (3.3), and (3.4) would be adequate [14].

We write h the size of the coarse mesh. Elements ψ_i are obtained by solving (3.6) on localized subdomains of size h_0. Table 6.1 shows errors with $\alpha = 1/2$ for a given by (6.1) (see [49, section 3, Example 1], trigonometric multiscale; see also [45]), i.e., for

TABLE 6.1
Example 1 of section 3 of [49] (trigonometric multiscale; see also [45]) with $\alpha = 1/2$.

h	L^2	H^1	L^∞
0.5	0.0119	0.0913	0.0157
0.25	0.0057	0.0664	0.0115
0.125	0.0027	0.0482	0.0075
0.0625	0.0005	0.0207	0.0032

$$a(x) := \frac{1}{6}\left(\frac{1.1+\sin(2\pi x/\epsilon_1)}{1.1+\sin(2\pi y/\epsilon_1)}+\frac{1.1+\sin(2\pi y/\epsilon_2)}{1.1+\cos(2\pi x/\epsilon_2)}+\frac{1.1+\cos(2\pi x/\epsilon_3)}{1.1+\sin(2\pi y/\epsilon_3)}\right.$$
$$\left.+\frac{1.1+\sin(2\pi y/\epsilon_4)}{1.1+\cos(2\pi x/\epsilon_4)}+\frac{1.1+\cos(2\pi x/\epsilon_5)}{1.1+\sin(2\pi y/\epsilon_5)}+\sin(4x^2y^2)+1\right), \tag{6.1}$$

where $\epsilon_1 = \frac{1}{5}$, $\epsilon_2 = \frac{1}{13}$, $\epsilon_3 = \frac{1}{17}$, $\epsilon_4 = \frac{1}{31}$, and $\epsilon_5 = \frac{1}{65}$.

Figure 6.1 shows the logarithm (in base 2) of the error with respect to $\log_2(h_0/h)$ (for $h = 0.125$) and the value of T used in (3.6) for a given by [49, section 3, Example 5] (percolation at criticality; the conductivity of each site is equal to γ or $1/\gamma$ with probability $1/2$ and $\gamma = 4$).

Figure 6.2 shows the logarithm (in base 2) of the error with respect to $\log_2(h_0/h)$ (for $h = 0.125$) and the value of T used in (3.6) for a given by [49, section 3, Example 3]; i.e., $a(x) = e^{h(x)}$, with $h(x) = \sum_{|k|\le R}(a_k \sin(2\pi k \cdot x) + b_k \cos(2\pi k \cdot x))$, where a_k and b_k are independent uniformly distributed random variables on $[-0.3, 0.3]$ and $R = 6$.

Remark 6.1. Two factors contribute to the error plots shown in Figures 6.1 and 6.2: a localization error that becomes dominant when h_0/h is small (i.e., the fact (2.6) is not solved over the whole domain Ω) and the distortion of the transfer property resulting from the $1/T$ term in (3.9). As expected, both figures show that when h_0/h is large, the error due to the distortion of the transfer property is dominant and is minimized by a

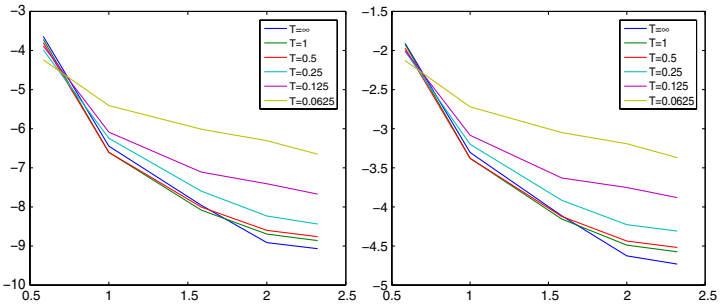

(a) L^2 error (b) H^1 error

FIG. 6.1. *Example* 5 *of section* 3 *of* [49] *(percolation at criticality). Logarithm (in base* 2*) of the error with respect to* $\log_2(h_0/h)$ *(for* $h = 0.125$*) and the value of* T *used in* (3.6).

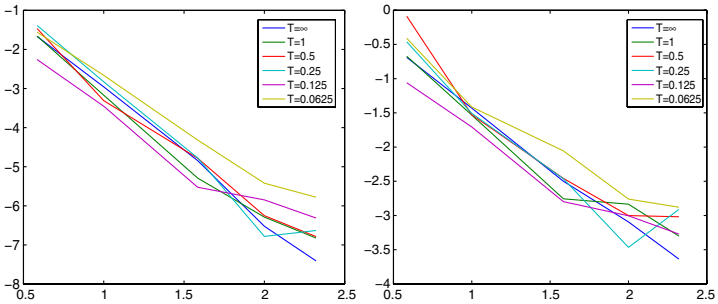

(a) L^2 error (b) H^1 error

FIG. 6.2. *Example* 3 *of section* 3 *of* [49] *(exponential of a sum of trigonometric functions with strongly overlapping frequencies). Logarithm (in base* 2*) of the error with respect to* $\log_2(h_0/h)$ *(for* $h = 0.125$*) and the value of* T *used in* (3.6).

large T. However, when h_0/h is small, the localization error is dominant and is minimized by a small T. The fact that in Figure 6.2 this error is minimized by the second smallest T instead of the smallest T is explained by the fact that the localization error remains bounded when h_0/h is of the order of one, whereas the error due to the distortion of the transfer property blows up as $T \downarrow 0$. The fact that in both figures curves associated with different T interest each other is indicative of the fact that for intermediate values of h_0/h, the error can be minimized via a fine-tuning of T as explained in section 3. The differences in the locations of these intersections can be explained by a larger localization error associated with the example of Figure 6.2 (due to longer correlation ranges). In particular, the comparison between Figures 6.1 and 6.2 indicates larger errors for Figure 6.2.

6.2. High contrast, with and without buffer. In this example, a is characterized by a fine and long-ranged high-conductivity channel (Figure 6.3). We choose $a(x) = 100$, if x is in the channel, and $a(x)$ is the percolation medium if x is not in the channel (the conductivity of each site not in the channel is equal to γ or $1/\gamma$ with probability $1/2$ and $\gamma = 4$). Figure 6.4 shows the $\log_2$ of the numerical error (in L^2 and H^1 norm) versus $\log_2(h)$. The three cases for the localization are $h_0 = \mathcal{O}(\sqrt{h}\ \ln\ \frac{1}{h})$ with a buffer b_i around the high-conductivity channel (see subsection 3.4) of size $\mathcal{O}(\sqrt{h}\ \ln\ \frac{1}{h})$, $h_0 = 3h$ with no buffer around the high-conductivity channel, and $h_0 = 3h$ with a buffer b_i around the high-conductivity channel of size $3h$. The first case shows that the method of subsection 3.4 is converging as expected. The second case shows that, as expected, taking $\alpha = 1$ does not guarantee convergence. The third case shows that adding a buffer around the high-conductivity channel improves numerical errors but is not sufficient to

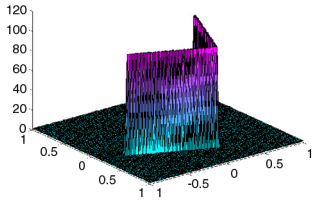

FIG. 6.3. *High-conductivity channel.*

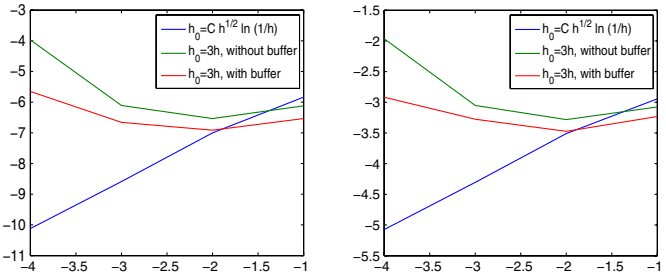

(a) L^2 ***error*** **(b)** H^1 ***error***

FIG. 6.4. *High-conductivity channel (Figure* 6.3*). The x-axis shows* $\log_2(h)$*, the y-axis shows the* $\log_2$ *of the error in* L^2 *and* H^1*-norm. The three cases for the localization are* $h_0 = \mathcal{O}(\sqrt{h}\ \ln\ \frac{1}{h})$ *with a buffer around the high-conductivity channel (see subsection* 3.4*) of size* $\mathcal{O}(\sqrt{h}\ \ln\ \frac{1}{h})$*,* $h_0 = 3h$ *with no buffer around the high-conductivity channel, and* $h_0 = 3h$ *with a buffer around the high-conductivity channel of size* $3h$*.*

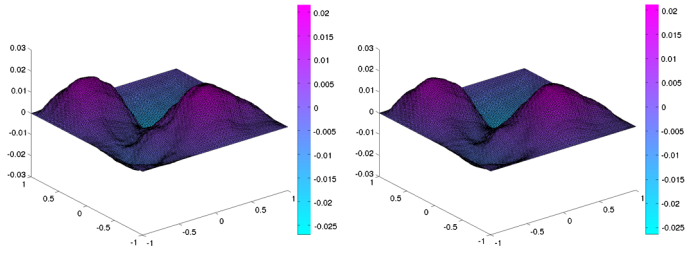

(a) u (b) u_h

FIG. 6.5. *Wave equation. Trigonometric case, fine mesh solution,* $h = 0.125$, $h_0 = 3h$, $T = h$. *The* L^2, H^1, *and* L^∞ *relative numerical errors are* 0.0339, 0.1760, *and* 0.0235.

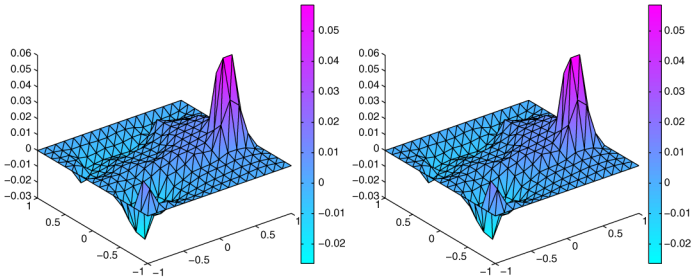

(a) u (b) u_h

FIG. 6.6. *Wave equation. Channel case, coarse mesh solution,* $h = 0.125$, $h_0 = 3h$, $T = h$. *The* L^2, H^1, *and* L^∞ *relative numerical errors are* 0.0439, 0.2684, *and* 0.0389.

guarantee convergence (as expected, we also need $\alpha < 1$). The percolating background medium has been resampled for each case; the effect of this resampling can be seen for the largest value of h (i.e., $\log_2(h) = -1$).

6.3. Wave equation. We compute the solutions of (5.1) up to time 1 on the fine mesh and in the finite-dimensional approximation space V_h defined in (3.7). The initial condition is $u(x,0) = 0$ and $u_t(x,0) = 0$. The boundary condition is $u(x,t) = 0$ for $x \in \partial\Omega$. The density is uniformly equal to one, and we choose $g = \sin(\pi x)\sin(\pi y)$. Figure 6.5 shows the fine mesh solutions u and u_h at time one, for a given by the trigonometric example (6.1), with $h = 0.125$, $h_0 = 3h$, and $T = h$. Figure 6.6 shows the coarse mesh solutions u and u_h at time one, for a given by the high-conductivity channel example (Figure 6.3), with $h = 0.125$, $h_0 = 3h$, and $T = h$.

We refer the reader to [52] for a list of movies on the numerical homogenization of the wave equation with and without high contrast and with and without buffers (extended buffers in the high-contrast case).

Appendix A. Proof of Proposition 3.2. The proof of Proposition 3.2 is a generalization of the proof of the control of the resonance error in periodic medium given in [35].

First we need the following lemma, which is the cornerstone of Cacciopoli's inequality.

LEMMA A.1. *Let* D *be a subdomain of* Ω *with piecewise Lipschitz boundary, and let* v *solve*

$$\begin{cases} \frac{v}{T} - \operatorname{div}(a(x)\nabla v(x)) = f(x), \quad x \in D; f \in H^{-1}(D), \\ v = 0 \quad \text{on } \partial D. \end{cases} \tag{A.1}$$

Let $\zeta : D \to \mathbb{R}^+$ be a function of class C^1 such that ζ is identically null on an open neighborhood of the support of f. Then,

$$\int_D |\nabla(\zeta v)|^2 \leq C \int_D v^2 |\nabla \zeta|^2, \tag{A.2}$$

where C only depends on the essential supremum and infimum of the maximum and minimum eigenvalues of a over D.

Proof. Multiplying (A.1) by $\zeta^2 v$ and integrating by parts, we obtain that

$$\int_D \zeta \frac{v^2}{T} + \int_D \nabla(\zeta^2 v) a \nabla v = 0. \tag{A.3}$$

Hence,

$$\int_D \zeta \frac{v^2}{T} + \int_D \nabla(\zeta v) a \nabla(\zeta v) = \int_D v^2 \nabla \zeta a \nabla \zeta, \tag{A.4}$$

which concludes the proof. ∎

LEMMA A.2. *Let D be a subdomain of Ω with piecewise Lipschitz boundary. Write $G_{T,D}$ for the Green's function of the operator $\frac{1}{T} - \operatorname{div}(a\nabla)$ with Dirichlet boundary condition on ∂D. Then,*

$$G_{T,D}(x,y) \leq \frac{C}{|x-y|^{d-2}} \exp\left(-\frac{|x-y|}{C\sqrt{T}}\right), \tag{A.5}$$

where C only depends on d and the essential supremum and infimum of the maximum and minimum eigenvalues of a over D.

Proof. Extending a to $\mathbb{R}^d$ and using the maximum principle, we obtain that

$$G_{T,D}(x,y) \leq G_{T,\mathbb{R}^d}(x,y); \tag{A.6}$$

we conclude by using the exponential decay of the Green's function in $\mathbb{R}^d$ (we refer the reader to Lemma 2 of [35]). ∎

LEMMA A.3. *Let $\psi_{i,T}$ be the solution of (3.9) and ψ_{i,T,Ω_i} the solution of (3.20). Let Ω_i' be a subdomain of Ω_i such that $S_i \subset \Omega_i'$ and $\operatorname{dist}(S_i, \Omega_i / \Omega_i') > 0$. We have*

$$\|\psi_{i,T}\|_{H^1(\Omega/\Omega_i')} \leq \frac{C h^{\frac{d}{2}-1}}{(\operatorname{dist}(S_i, \Omega/\Omega_i'))^d} \exp\left(-\frac{\operatorname{dist}(S_i, \Omega/\Omega_i')}{C\sqrt{T}}\right), \tag{A.7}$$

and

$$\|\psi_{i,T,\Omega_i}\|_{H^1(\Omega_i/\Omega_i')} \leq \frac{C h^{\frac{d}{2}-1}}{(\operatorname{dist}(S_i, \Omega/\Omega_i'))^d} \exp\left(-\frac{\operatorname{dist}(S_i, \Omega/\Omega_i')}{C\sqrt{T}}\right). \tag{A.8}$$

Proof. For $A \subset \Omega$, write A^r for the set of points of Ω that are at distance at most r from A. Let us now use Cacciopoli's inequality to bound $\int_{\Omega/\Omega_i'} |\nabla \psi_{i,T}|^2$. Using

Lemma A.1 with ζ identically equal to one on Ω/Ω_i', zero on $(\Omega/\Omega_i')^r$ with $r := \operatorname{dist}(S_i, \Omega/\Omega_i')/3$, and $|\nabla\zeta| \le C/r$, we obtain that

$$\int_{\Omega/\Omega_i'} |\nabla\psi_{i,T}|^2 \le \frac{C}{r^2}\int_{(\Omega/\Omega_i')^r} \psi_{i,T}^2. \tag{A.9}$$

Next, observe that for $x \in (\Omega/\Omega_i')^r$,

$$\psi_{i,T}(x) = -\int_{S_i} \nabla G_{T,\Omega}(x,y)\nabla\varphi_i(y)\,dy. \tag{A.10}$$

Hence,

$$|\psi_{i,T}(x)| \le \|\nabla\varphi_i\|_{(L^2(S_i))^d}\|\nabla G_{T,\Omega}(x,.)\|_{(L^2(S_i))^d}. \tag{A.11}$$

Another use of Cacciopoli's inequality leads to

$$\|\nabla G_{T,\Omega}(x,.)\|_{(L^2(S_i))^d} \le \frac{C}{r}\|G_{T,\Omega}(x,.)\|_{L^2(S_i^r)}. \tag{A.12}$$

Combining (A.9) with (A.11) and (A.12), we obtain that

$$\int_{\Omega/\Omega_i'} |\nabla\psi_{i,T}|^2 \le \|\nabla\varphi_i\|^2_{(L^2(S_i))^d}\frac{C}{r^4}\int_{(\Omega/\Omega_i')^r} \|G_{T,\Omega}(x,.)\|^2_{L^2(S_i^r)}. \tag{A.13}$$

We conclude the proof of (A.7) using Lemma A.2 and (3.3). The proof of (A.8) is similar observing that $\operatorname{dist}(S_i, \Omega/\Omega_i') \le \operatorname{dist}(S_i, \Omega_i/\Omega_i')$. ∎

Lemma A.4. *Let D be a subdomain of Ω with piecewise Lipschitz boundary. Let $\psi \in H^1(\Omega)$, and let v solve*

$$\begin{cases} \frac{v}{T} - \operatorname{div}(a(x)\nabla v(x)) = 0, & x \in D, \\ v = \psi \quad \text{on } \partial D. \end{cases} \tag{A.14}$$

Write S for the intersection of the support of ψ with D. Let D_1 be a subdomain of D such that $\operatorname{dist}(D_1, S) > 0$; then

$$\int_{D_1} |\nabla v|^2 \le \frac{C}{(\operatorname{dist}(D_1,S))^{2d}}(T^{-1}+1)^2\|\psi\|^2_{H^1(\Omega)}\exp\left(-\frac{\operatorname{dist}(D_1,S)}{C\sqrt{T}}\right), \tag{A.15}$$

where C does not depend on D, D_1, or S.

Proof. Write $w := v - \psi$. Then,

$$\begin{cases} \frac{w}{T} - \operatorname{div}(a(x)\nabla w(x)) = -\frac{\psi}{T} + \operatorname{div}(a\nabla\psi), & x \in D, \\ v = 0 \quad \text{on } \partial D. \end{cases} \tag{A.16}$$

Thus,

$$w(x) = -\int_D \left(\frac{\psi(y)}{T}\,G_{T,D}(x,y) + \nabla\psi(y)a(y)\nabla G_{T,D}(x,y)\right)dy. \tag{A.17}$$

Using the Cauchy–Schwarz inequality, we obtain that

$$|w(x)| \leq C\|\psi\|_{H^1(\Omega)}\left(\frac{1}{T}\|G_{T,D}(x,.)\|_{L^2(S)} + \|\nabla G_{T,D}(x,.)\|_{(L^2(S))^d}\right). \tag{A.18}$$

For $A \subset D$, write A^r for the set of points of D that are at distance at most r from A. Let us now use Cacciopoli's inequality to bound $\int_{D_1}|\nabla w|^2$. Using Lemma A.1 with ζ identically equal to one on D_1, zero on $D/D_1^{r_1}$, and such that $|\nabla\zeta| \leq C/r_1$, we obtain that

$$\int_{D_1}|\nabla w|^2 \leq \frac{C}{r_1^2}\int_{D_1^{r_1}} w^2, \tag{A.19}$$

provided that $\operatorname{dist}(D_1^{r_1}, S) > 0$. Hence, for $r_1 \coloneqq \operatorname{dist}(D_1, S)/3$, we obtain (A.19). Taking $r_2 \coloneqq \operatorname{dist}(D_1, S)/3$ and using Cacciopoli's inequality again, we also obtain that

$$\|\nabla G_{T,D}(x,.)\|_{(L^2(S))^d} \leq \frac{C}{r_2}\|G_{T,D}(x,.)\|_{L^2(S^{r_2})}. \tag{A.20}$$

Combining (A.19) with (A.18) and (A.20) and observing that $w = v$ on $D_1^{r_1}$, we obtain that

$$\int_{D_1}|\nabla v|^2 \leq \frac{C}{r_1^2 r_2^2}\|\psi\|^2_{H^1(\Omega)}(T^{-1}+1)^2\int_{D_1^{r_1}}\|G_{T,D}(x,.)\|^2_{L^2(S^{r_2})}. \tag{A.21}$$

Using Lemma A.2, we deduce that

$$\int_{D_1}|\nabla w|^2 \leq \frac{C|\Omega|}{(\operatorname{dist}(D_1,S))^{2d}}\|\psi\|^2_{H^1(\Omega)}(T^{-1}+1)^2\exp\left(-\frac{\operatorname{dist}(D_1,S)}{C\sqrt{T}}\right). \tag{A.22}$$

This concludes the proof of Lemma A.4. ∎

LEMMA A.5. *Let $\psi_{i,T}$ be the solution of* (3.9) *and ψ_{i,T,Ω_i} the solution of* (3.20). *Let Ω_i' be a subdomain of Ω_i such that* $\operatorname{dist}(\Omega/\Omega_i, \Omega_i') > 0$. *We have*

$$\|\psi_{i,T} - \psi_{i,T,\Omega_i}\|_{H^1(\Omega_i')} \leq \frac{C(T^{-1}+1)h^{\frac{d}{2}-1}}{(\operatorname{dist}(\Omega/\Omega_i,\Omega_i'))^{d+1}}\exp\left(-\frac{\operatorname{dist}(\Omega/\Omega_i,\Omega_i')}{C\sqrt{T}}\right). \tag{A.23}$$

Proof. Lemma A.5 is a direct consequence of Lemma A.4. To this end, we choose $D \coloneqq \Omega_i$, $v =: \psi_{i,T} - \psi_{i,T,\Omega_i}$, and $D_1 \coloneqq \Omega_i'$. We also choose $\psi \coloneqq \eta\psi_{i,T}$, where $\eta : \Omega \to [0,1]$ is C^1, equal to one on Ω/Ω_i and 0 on $(\Omega/\Omega_i)^r$ with $r \coloneqq \operatorname{dist}(\Omega/\Omega_i,\Omega_i')/3$ (A^r being the set of points in Ω at distance at most r from A), and $|\nabla\eta| \leq C/r$. We obtain from Lemma A.4 that

$$\|\psi_{i,T} - \psi_{i,T,\Omega_i}\|_{H^1(\Omega_i')} \leq \frac{C(T^{-1}+1)}{(\operatorname{dist}(\Omega/\Omega_i,\Omega_i'))^d}\|\psi\|_{H^1(\Omega)}\exp\left(-\frac{\operatorname{dist}(\Omega/\Omega_i,\Omega_i')}{C\sqrt{T}}\right). \tag{A.24}$$

We conclude using (3.3) and $\|\psi\|_{H^1(\Omega)} \leq \frac{C}{\operatorname{dist}(\Omega/\Omega_i,\Omega_i')}\|\nabla\varphi_i\|_{(L^2(\Omega))^d}$. ∎

Observing that

$$\|\psi_{i,T} - \psi_{i,T,\Omega_i}\|_{H^1(\Omega)} \leq \|\psi_{i,T} - \psi_{i,T,\Omega_i}\|_{H^1(\Omega_i')} + \|\psi_{i,T}\|_{H^1(\Omega/\Omega_i')} + \|\psi_{i,T,\Omega_i}\|_{H^1(\Omega_i/\Omega_i')}, \tag{A.25}$$

we conclude the proof of Proposition 3.2 by using Lemma A.5 and Lemma A.3 with $\mathbf{\Omega}_i' \coloneqq S_i^r$, where S_i^r are the points in $\mathbf{\Omega}_i$ at distance at most r from S_i with $r \coloneqq \operatorname{dist}(S_i, \mathbf{\Omega}/\mathbf{\Omega}_i)/3$.

Appendix B. On the compactness of the solution space. Although the foundations of classical homogenization [9] were laid down based on assumptions of periodicity (or ergodicity) and scale-separation, numerical homogenization, as described here, is independent from these concepts and solely relies on the strong compactness of the solution space (and the fact that a compact set can be covered with a finite number of balls of arbitrary sizes). Observe that an analogous notion of compactness supports the foundations of G- and H-convergence (see [47], [57], [32]). The main difference is that G- and H-convergence rely on precompactness and weak convergence of fluxes, and here, we rely on compactness in the (strong) H_0^1-norm, i.e., the following theorem.

Let W be the range of g in (1.1). Write

$$V \coloneqq \{u \in H_0^1(\mathbf{\Omega}) : u \text{ solves (1.1) for some } g \in W\}. \tag{B.1}$$

THEOREM B.1. *Let $\nu < 1$. If W is a closed bounded subset of $H^{-\nu}(\mathbf{\Omega})$, then W is a compact subset of $H_0^1(\mathbf{\Omega})$ (in the strong H_0^1-norm).*

Proof. We have $(a\nabla u)_{\text{pot}} = -\nabla\Delta^{-1}g$. So using the same notation as in (2.4), we get $(a\nabla V)_{\text{pot}} = -\nabla\Delta^{-1}W$. Let u_n be a sequence in V; then there exists a sequence in W such that $-\operatorname{div}(a\nabla u_n) = g_n$. Using the fact that $-\nabla\Delta^{-1}W$ is a compact subset of $(L^2(\mathbf{\Omega}))^d$ (we refer, for instance, to the Kondrachov embedding theorem), we get that there exists $g^* \in W$ such that $\|\nabla\Delta^{-1}g_n - \nabla\Delta^{-1}g^*\|_{L^2} \to 0$. Writing u^* for the solution of $-\operatorname{div}(a\nabla u^*) = g^*$ and using $(a\nabla(u_n - u^*))_{\text{pot}} = -\nabla\Delta^{-1}(g_n - g^*)$, we get that $\|(a\nabla(u_n - u^*))_{\text{pot}}\|_{L^2} \to 0$. Using the equivalence between the flux-norm and the H_0^1 norm we deduce that $\|u_n - u^*\|_{H_0^1} \to 0$. This finishes the proof. ∎

This notion of compactness of the solution space constitutes a simple but fundamental link between classical homogenization, numerical homogenization, and reduced order modeling (or reduced basis modeling [20], [43]) (we also refer the reader to the discussion in section 6 of [10]). This notion is also what allows for atomistic to continuum upscaling [64]; the basic idea is that if source (force) terms are integrable enough (for instance, in L^2 instead of H^{-1}), then the solution space is no longer H^1 but a subspace V that is compactly embedded into H^1, and, hence, it can be approximated by a finite-dimensional space (in the H^1-norm). In other words, if these systems are "excited" by "regular" forces or source terms (think compact, low dimensional), then the solution space can be approximated by a low dimensional space (of the whole space), and the name of the game becomes "how to approximate" this solution space (and this can be done by using local time-independent solutions).

Acknowledgments. We thank L. Berlyand for stimulating discussions. We also thank Ivo Babuška, John Osborn, George Papanicolaou, and Björn Engquist for pointing us in the direction of the localization problem. Finally, we thank Sydney Garstang for proofreading the manuscript.

REFERENCES

[1] A. ABDULLE AND M. J. GROTE, *Finite element heterogeneous multiscale method for the wave equation*, Multiscale Model. Simul., 9 (2011), pp. 766–792.

[2] G. ALLAIRE AND R. BRIZZI, *A multiscale finite element method for numerical homogenization*, Multiscale Model. Simul., 4 (2005), pp. 790–812.

[3] T. Arbogast and K. J. Boyd, *Subgrid upscaling and mixed multiscale finite elements*, SIAM J. Numer. Anal., 44 (2006), pp. 1150–1171.
[4] T. Arbogast, C.-S. Huang, and S.-M. Yang, *Improved accuracy for alternating-direction methods for parabolic equations based on regular and mixed finite elements*, Math. Models Methods Appl. Sci., 17 (2007), pp. 1279–1305.
[5] I. Babuška, G. Caloz, and J. E. Osborn, *Special finite element methods for a class of second order elliptic problems with rough coefficients*, SIAM J. Numer. Anal., 31 (1994), pp. 945–981.
[6] I. Babuška and R. Lipton, *Optimal local approximation spaces for generalized finite element methods with application to multiscale problems*, Multiscale Model. Simul., 9 (2011), pp. 373–406.
[7] I. Babuška and J. E. Osborn, *Generalized finite element methods: Their performance and their relation to mixed methods*, SIAM J. Numer. Anal., 20 (1983), pp. 510–536.
[8] G. Bal and W. Jing, *Corrector theory for msfem and hmm in random media*, Multiscale Model. Simul., to appear.
[9] A. Bensoussan, J.-L. Lions, and G. Papanicolaou, *Asymptotic Analysis for Periodic Structure*, North–Holland, Amsterdam, 1978.
[10] L. Berlyand and H. Owhadi, *Flux norm approach to finite dimensional homogenization approximations with non-separated scales and high contrast*, Arch. Ration. Mech. Anal., 198 (2010), pp. 677–721.
[11] C. Bernardi and R. Verfürth, *Adaptive finite element methods for elliptic equations with non-smooth coefficients*, Numer. Math., 85 (2000), pp. 579–608.
[12] X. Blanc, C. Le Bris, and P.-L. Lions, *Une variante de la théorie de l'homogénéisation stochastique des opérateurs elliptiques*, C. R. Math. Acad. Sci. Paris, 343 (2006), pp. 717–724.
[13] X. Blanc, C. Le Bris, and P.-L. Lions, *Stochastic homogenization and random lattices*, J. Math. Pures Appl. (9), 88 (2007), pp. 34–63.
[14] D. Braess, *Finite Elements: Theory, Fast Solvers, and Applications in Solid Mechanics*, Cambridge University Press, London, 2007.
[15] A. Braides, Γ-*Convergence for Beginners*, Oxford Lecture Ser. Math. Appl. 22, Oxford University Press, Oxford, 2002.
[16] L. V. Branets, S. S. Ghai, S. L. Lyons, and X.-H. Wu, *Challenges and technologies in reservoir modeling*, Commun. Comput. Phys., 6 (2009), pp. 1–23.
[17] S. C. Brenner and L. R. Scott, *The Mathematical Theory of Finite Element Methods*, 2nd ed., Texts Appl. Math. 15, Springer, New York, 2002.
[18] D. L. Brown, *A note on the numerical solution of the wave equation with piecewise smooth coefficients*, Math. Comp., 42 (1984), pp. 369–391.
[19] L. A. Caffarelli and P. E. Souganidis, *A rate of convergence for monotone finite difference approximations to fully nonlinear, uniformly elliptic PDEs*, Comm. Pure Appl. Math., 61 (2008), pp. 1–17.
[20] E. Cancès, C. Le Bris, Y. Maday, N. C. Nguyen, A. T. Patera, and G. S. H. Pau, *Feasibility and competitiveness of a reduced basis approach for rapid electronic structure calculations in quantum chemistry*, in High-Dimensional Partial Differential Equations in Science and Engineering, CRM Proc. Lecture Notes 41, AMS, Providence, RI, 2007, pp. 15–47.
[21] K. D. Cherednichenko, V. P. Smyshlyaev, and V. V. Zhikov, *Non-local homogenized limits for composite media with highly anisotropic periodic fibres*, Proc. Roy. Soc. Edinburgh Sect. A, 136 (2006), pp. 87–114.
[22] C.-C. Chu, I. G. Graham, and T. Y. Hou, *A new multiscale finite element method for high-contrast elliptic interface problems*, Math. Comp., 79 (2010), pp. 1915–1955.
[23] A. Doostan and H. Owhadi, *A non-adapted sparse approximation of pdes with stochastic inputs*, J. Comput. Phys., 230 (2011), pp. 3015–3034.
[24] W. E, B. Engquist, X. Li, W. Ren, and E. Vanden-Eijnden, *Heterogeneous multiscale methods: A review*, Commun. Comput. Phys., 2 (2007), pp. 367–450.
[25] Y. Efendiev, J. Galvis, and X. Wu, *Multiscale finite element and domain decomposition methods for high-contrast problems using local spectral basis functions*, J. Comput. Phys., 230 (2011), pp. 937–955.
[26] Y. Efendiev, V. Ginting, T. Hou, and R. Ewing, *Accurate multiscale finite element methods for two-phase flow simulations*, J. Comput. Phys., 220 (2006), pp. 155–174.
[27] Y. Efendiev and T. Hou, *Multiscale finite element methods for porous media flows and their applications*, Appl. Numer. Math., 57 (2007), pp. 577–596.
[28] B. Engquist, H. Holst, and O. Runborg, *Multi-scale methods for wave propagation in heterogeneous media*, Commun. Math. Sci., 9 (2011), pp. 33–56.
[29] B. Engquist and P. E. Souganidis, *Asymptotic and numerical homogenization*, Acta Numer., 17 (2008), pp. 147–190.

[30] B. Engquist and L. Ying, *Sweeping preconditioner for the Helmholtz equation: Hierarchical matrix representation*, Comm. Pure Appl. Math., 64 (2011), pp. 697–735.
[31] B. Engquist and L. Ying, *Sweeping preconditioner for the Helmholtz equation: Moving perfectly matched layers*, Multiscale Model. Simul., 9 (2011), pp. 686–710.
[32] E. D. Giorgi, *Sulla convergenza di alcune successioni di integrali del tipo dell'aera*, Rend. Mat. Appl. (7), 8 (1975), pp. 277–294.
[33] E. D. Giorgi, *New problems in* Γ*-convergence and G-convergence*, in Free Boundary Problems, Vol. II, Ist. Naz. Alta Mat. Francesco Severi, Rome, 1980, pp. 183–194.
[34] A. Gloria, *An analytical framework for the numerical homogenization of monotone elliptic operators and quasiconvex energies*, Multiscale Model. Simul., 5 (2006), pp. 996–1043.
[35] A. Gloria, *Reduction of the resonance error. Part* 1*: Approximation of homogenized coefficients*, Math. Models Methods Appl. Sci., 21 (2011), pp. 1601–1630.
[36] A. Gloria and F. Otto, *An optimal error estimate in stochastic homogenization of discrete elliptic equations*, Ann. Appl. Probab., to appear.
[37] H. Harbrecht, R. Schneider, and C. Schwab, *Sparse second moment analysis for elliptic problems in stochastic domains*, Numer. Math., 109 (2008), pp. 385–414.
[38] K. Höllig, *Finite Element Methods with B-Splines*, Frontiers Appl. Math. 26, SIAM, Philadelphia, PA, 2003.
[39] K. Höllig, U. Reif, and J. Wipper, *Weighted extended B-spline approximation of Dirichlet problems*, SIAM J. Numer. Anal., 39 (2001), pp. 442–462.
[40] T. Y. Hou and X.-H. Wu, *A multiscale finite element method for elliptic problems in composite materials and porous media*, J. Comput. Phys., 134 (1997), pp. 169–189.
[41] T. Y. Hou, X.-H. Wu, and Z. Cai, *Convergence of a multiscale finite element method for elliptic problems with rapidly oscillating coefficients*, Math. Comp., 68 (1999), pp. 913–943.
[42] S. M. Kozlov, *The averaging of random operators*, Mat. Sb., 109 (1979), pp. 188–202.
[43] L. Machiels, Y. Maday, I. B. Oliveira, A. T. Patera, and D. V. Rovas, *Output bounds for reduced-basis approximations of symmetric positive definite eigenvalue problems*, C. R. Math. Acad. Sci. Paris, 331 (2000), pp. 153–158.
[44] J. M. Melenk, *On n-widths for elliptic problems*, J. Math. Anal. Appl., 247 (2000), pp. 272–289.
[45] P. Ming and X. Yue, *Numerical methods for multiscale elliptic problems*, J. Comput. Phys., 214 (2006), pp. 421–445.
[46] F. Murat, *Compacité par compensation*, Ann. Scuola Norm. Sup. Pisa Cl. Sci., 5 (1978), pp. 489–507.
[47] F. Murat and L. Tartar, *H-convergence*, Séminaire d'Analyse Fonctionnelle et Numérique de l'Université d'Alger, 1978.
[48] J. Nolen, G. Papanicolaou, and O. Pironneau, *A framework for adaptive multiscale methods for elliptic problems*, Multiscale Model. Simul., 7 (2008), pp. 171–196.
[49] H. Owhadi and L. Zhang, *Metric-based upscaling*, Comm. Pure Appl. Math., 60 (2007), pp. 675–723.
[50] H. Owhadi and L. Zhang, *Homogenization of parabolic equations with a continuum of space and time scales*, SIAM J. Numer. Anal., 46 (2007), pp. 1–36.
[51] H. Owhadi and L. Zhang, *Homogenization of the acoustic wave equation with a continuum of scales*, Comput. Methods Appl. Mech. Engrg., 198 (2008), pp. 97–406.
[52] H. Owhadi and L. Zhang, *Numerical Homogenization with Localized Bases*, http://www.youtube.com/view_play_list?p=2009D30DF7B07294 (2010).
[53] G. C. Papanicolaou and S. R. S. Varadhan, *Boundary value problems with rapidly oscillating random coefficients*, in Random Fields, Vol. I, II, Colloq. Math. Soc. János Bolyai 27, North–Holland, Amsterdam, 1981, pp. 835–873.
[54] A. Pinkus, *n-Width in Approximation Theory*, Springer, New York, 1985.
[55] A. Pinkus, *n-Widths in Approximation Theory*, Ergebnisse der Mathematik und ihrer Grenzgebiete (3) [Results in Mathematics and Related Areas (3)] 7, Springer, Berlin, 1985.
[56] A. Sei and W. W. Symes, *Error analysis of numerical schemes for the wave equation in heterogeneous media*, Appl. Numer. Math., 15 (1994), pp. 465–480.
[57] S. Spagnolo, *Sulla convergenza di soluzioni di equazioni paraboliche ed ellittiche.*, Ann. Sc. Norm. Super. Pisa Cl. Sci. (5), 22 (1968), pp. 571–597.
[58] S. Spagnolo, *Convergence in energy for elliptic operators*, in Numerical Solution of Partial Differential Equations, III, Academic Press, New York, 1976, pp. 469–498.
[59] W. W. Symes and T. Vdovina, *Interface error analysis for numerical wave propagation*, Comput. Geosci., 13 (2009), pp. 363–371.

[60] R. A. Todor and C. Schwab, *Convergence rates for sparse chaos approximations of elliptic problems with stochastic coefficients*, IMA J. Numer. Anal., 27 (2007), pp. 232–261.

[61] C. D. White and R. N. Horne, *Computing absolute transmissibility in the presence of finescale heterogeneity*, in Proceedings of the SPE Symposium on Reservoir Simulation, 1987, p. 16011.

[62] X. H. Wu, Y. Efendiev, and T. Y. Hou, *Analysis of upscaling absolute permeability*, Discrete Contin. Dyn. Syst. Ser. B, 2 (2002), pp. 185–204.

[63] V. V. Yurinskii, *Averaging of symmetric diffusion in a random medium*, Sibirsk. Mat. Zh., 27 (1986), pp. 167–180.

[64] L. Zhang, L. Berlyand, M. Federov, and H. Owhadi, *Global energy matching method for atomistic-to-continuum modeling of self-assembling biopolymer aggregates*, Multiscale Model. Simul., 8 (2010), pp. 1958–1980.